# The Use of GPC Coupled with a Multiangle Laser Light Scattering Photometer for the Characterization of Polymers. On the Determination of Molecular Weight, Size, and Branching

## S. PODZIMEK*

Institute for Organic and Macromolecular Chemistry, Heinrich Heine University, 40225 Düsseldorf, Germany

### SYNOPSIS

The use of gel permeation chromatography (GPC) coupled with the multiangle laser light scattering (MALLS) detector for the determination of molecular weight and size distribution and for the identification of polymer branching is demonstrated on several examples of both organic and water soluble polymers. The influence of the second virial coefficient and the way of the light scattering data evaluation on the results obtained is shown. Measurements of the root mean square radius are presented for two series of polystyrene and polymethylmethacrylate standards, and the results are compared with the radii calculated from the Flory-Fox equation. © 1994 John Wiley & Sons, Inc.

## INTRODUCTION

GPC has become the most widely employed method for the molecular weight characterization of polymers. In its conventional form, the method is equipped with a concentration sensitive detector (usually differential refractometer) monitoring the solute concentration in the effluent. To convert a GPC chromatogram to molecular weight distribution, GPC columns must be calibrated, i.e., the relation between molecular weight and elution volume must be determined for each polymer to be analyzed. The determination of a reliable calibration for a particular polymer is usually the basic problem of GPC. Coupling the GPC instrument with a molecular weight sensitive light-scattering photometer overcomes this problem at least for homopolymers. In the seventies, low-angle laser light-scattering (LALLS) photometers were launched on the market. The MALLS detector, commercially introduced in the eighties, represents the most sophisticated detector for GPC today. The intention of this work

is to demonstrate the reliability of GPC-MALLS and to show various possibilities of the method.

## THEORETICAL BACKGROUND

The fundamental theory of light scattering from macromolecular solutions is given by the works of Debye and Zimm.[1-3] The theoretical basis and some details about instrumental equipment together with several experimental results have been reviewed by Wyatt.[4] Comprehensible information about light scattering from polymer solutions can be found in Kratochvíl's monograph.[5] A computer simulation study of some problems of GPC with light scattering and viscosity detectors has been reported by Jackson and Yau.[6] Analysis of the accuracy of determination of molecular weight distribution by the GPC with the on-line light scattering detector has been done by Procházka and Kratochvíl.[7,8]

The intensity of light scattered from a volume unit of a diluted macromolecular solution at angle $\Theta$ is given by equation:

$$\frac{R_\Theta}{Kc} = MP(\Theta) - 2A_2cM^2P^2(\Theta) + \cdots \quad (1)$$

where $R_\Theta$ is the excess Rayleigh ratio, $P(\Theta)$ is the particle scattering function, $c$ is the concentration of polymer molecules (g/mL), $M$ is the molecular weight (the weight-average molecular weight $M_w$ must be used instead of $M$ in the case of polydisperse sample), $A_2$ is the second virial coefficient (mL mol/ g$^2$). $K$ is a constant that is for vertically polarized incident light given by:

$$K = \frac{4\pi^2 n_0^2}{\lambda_0^4 N_A}\left(\frac{dn}{dc}\right)^2 \quad (2)$$

where $n_0$ is the refractive index of the solvent at the given wavelength, $\lambda_0$ is the wavelength of the incident radiation in vacuum, $N_A$ is Avogadro's number, $dn/dc$ is the specific refractive index increment of the polymer in a given solvent that can be found in the literature[9,10] or measured beforehand in a separate experiment.

Excess Rayleigh ratio (compared to that of the solvent alone) is defined as:

$$R_\Theta = \frac{(I_\Theta - I_{\Theta,\text{solvent}})r^2}{I_0 V} = f \times \frac{I_\Theta - I_{\Theta,\text{solvent}}}{I_0} \quad (3)$$

where $I_\Theta$ is the intensity of light, i.e., amount of energy passing in unit time through unit area, scattered in the direction at an angle $\Theta$ to the incident light beam. $I_0$ is the intensity of the primary beam, $I_{\Theta,\text{solvent}}$ is the scattered intensity of the solvent, $V$ is the volume of the scattered solution, $r$ is the distance between the scattering volume and the detector, and $f$ is a calibration constant derived from the geometry of the instrument. The dimension of $R_\Theta$ is (length)$^{-1}$, usually cm$^{-1}$.

The second virial coefficient is a measure of the thermodynamic quality of the solvent for a given polymer. High positive values of $A_2$ are characteristic for thermodynamically good solvents. For a great number of polymer-solvent systems the value of $A_2$ decreases with increasing molecular weight according to the relationship:

$$A_2 = \text{constant} \times M^{-\theta} \quad (4)$$

The higher $A_2$, the better is the thermodynamic quality of the solvent for the given polymer. Equation (4) explaines why the polymers with higher molecular weights dissolve less readily then chemically identical polymers with lower $M$. The typical values of $\theta$ are 0.15 to 0.35. The values of $A_2$ can be found in the literature[9] or may be measured for the bulk sample using standard Zimm plot technique with the DAWN photometer. The particle scattering

function (also called the particle scattering factor) $P(\Theta)$ describes the angular dependence of the intensity of scattered light. The definition of the particle scattering function is:

$$P(\Theta) = \frac{R_\Theta}{R_0} \quad (5)$$

where $R_\Theta$ and $R_0$ are the excess Raileigh ratios at the angle of observation $\Theta$ and zero, respectively. For small molecules (maximum distance between two points of a particle does not exceed approximately $\lambda/20$), the angular dependence of the scattered light intensity becomes negligible and $P(\Theta) = 1$ for all angles of observation. The important property of $P(\Theta)$ is that it is a function of particle size:

$$P(\Theta) = 1 - \frac{16\pi^2}{3\lambda^2}\sin^2\left(\frac{\Theta}{2}\right)\langle r_g^2\rangle + \cdots \quad (6)$$

or for $\Theta \to 0$

$$P^{-1}(\Theta) = 1 + \frac{16\pi^2}{3\lambda^2}\sin^2\left(\frac{\Theta}{2}\right)\langle r_g^2\rangle \quad (7)$$

where $\lambda$ is the wavelength of the incident light in a given solvent ($\lambda = \lambda_0/n_0$), $\langle r_g^2\rangle$ is the mean square (MS) radius.

The root mean square (RMS) radius $\langle r_g^2\rangle^{1/2}$ (often called the radius of gyration) describes the size of a macromolecular particle in a solution, regardless of its shape. After the separation of the particle to $N$ small elements of identical mass, the RMS radius is defined as follows:

$$r_g = \left(\frac{1}{N}\sum_{i=1}^{N} r_i^2\right)^{1/2} \quad (8)$$

where $r_i^2$ is the square distance of the $i$-th element from the center of gravity. For a flexible chain, each conformation has a different $r_g$ and, hence, only the average of $r_g$ over all conformations has practical meaning:

$$\langle r_g^2\rangle^{1/2} = \left(\frac{1}{N}\sum_{i=1}^{N}\langle r_i^2\rangle\right)^{1/2} \quad (9)$$

where $\langle r_i^2\rangle$ is the average square distance of the $i$-th mass element from the center of gravity over all conformations and $\langle r_g^2\rangle^{1/2}$ is the RMS radius usually expressed in nm. It is important to note that RMS radius is not identical with geometrical radius.

Equation (1) may be put into a reciprocal form more linear in $\sin^2(\Theta/2)$:

$$\frac{Kc}{R_\Theta} = \frac{1}{MP(\Theta)} + 2A_2c + \cdots \qquad (10)$$

The experiments are usually carried out at sufficiently low concentrations, where the terms with higher powers of concentration in Eqs. (1) and (10) can be neglected. Equation (1) is the basis of the calculation in ASTRA (i.e., Wyatt software designed for the use with the DAWN photometer), but calculation according to Eq. (10) may be also carried out employing the special ASTRA module. To determine the molecular weight and RMS radius distribution, the sample concentration for each data slice is determined from the concentration detector output, and $R_\Theta/Kc$ (or $Kc/R_\Theta$) vs. $\sin^2(\Theta/2)$ plot is constructed and the intercept at zero angle $R_0/Kc$ $(Kc/R_0)$, as well as the slope at zero angle $m_0 = d[R_\Theta/Kc]/d[\sin^2(\Theta/2)]$ $(d[Kc/R_\Theta]/d[\sin^2(\Theta/2)])$ are determined. For zero angle, $P(\Theta)$ approaches unity and the molecular weight and RMS radius can be extracted from Eq. (1) or (10). For example, solving Eq. (10) for $M$ yields:

$$M = \left(\frac{Kc}{R_0} - 2A_2c\right)^{-1} \qquad (11)$$

or if $A_2 = 0$

$$M = \left(\frac{Kc}{R_0}\right)^{-1} \qquad (12)$$

and for $\langle r_g^2 \rangle^{1/2}$:

$$\langle r_g^2 \rangle^{1/2} = \frac{\sqrt{3}\lambda_0}{4\pi n_0} \sqrt{m_0 M} \qquad (13)$$

Once the concentration $c_i$, molecular weight $M_i$, and MS radius $\langle r_g^2 \rangle_i$ have been determined for each slice along the entire GPC chromatogram, the molecular weight and MS radius moments can be calculated from the following relationships:

Number-average molecular weight

$$M_n = \frac{\sum c_i}{\sum c_i/M_i} \qquad (14)$$

Weight-average molecular weight

$$M_w = \frac{\sum c_i M_i}{\sum c_i} \qquad (15)$$

$z$-average molecular weight $M_z = \dfrac{\sum c_i M_i^2}{\sum c_i M_i}$ $\quad$ (16)

Number-average MS radius

$$\langle r_g^2 \rangle_n = \frac{\sum \langle r_g^2 \rangle_i c_i/M_i}{\sum c_i/M_i} \qquad (17)$$

Weight-average MS radius

$$\langle r_g^2 \rangle_w = \frac{\sum \langle r_g^2 \rangle_i c_i}{\sum c_i} \qquad (18)$$

$z$-average MS radius $\langle r_g^2 \rangle_z = \dfrac{\sum \langle r_g^2 \rangle_i c_i M_i}{\sum c_i M_i}$ $\quad$ (19)

Because of peak broadening in a GPC instrument, each slice contains a mixture of species. Due to this effect, the quantities $M_i$ and $\langle r_g^2 \rangle_i$ in the equations above are weight average and $z$ average, respectively. Consequently, GPC with light scattering detection has a tendency to overestimate $n$ averages. Nevertheless, in the high performance GPC, each slice may be assumed to contain molecules of very narrow distribution.

Sample concentration for each data slice is determined from the refractive index (RI) detector output. The determination of the sample concentration is done using one of three methods. The mass method calculates the concentration of solute in each slice from the injected mass for the peak, the sample RI detector signal voltage, and the volume of the slice. The RI detector constant (in RI units per volt) is used to calculate a value of $dn/dc$ which is subsequently used in the molecular weight calculations. The mass method does not require a value of $dn/dc$, but the total injected mass corresponding to the peak which is to be analyzed must be known. The $dn/dc$ method does not require a knowledge of the total injected mass, but does require values for both the RI detector instrument constant and the specific refractive index increment $dn/dc$. The solute concentration is calculated from the sample RI detector signal voltage, the RI detector constant and the value of $dn/dc$. The combined method uses the mass method to calculate the concentration for each data slice, but uses the $dn/dc$ method to calculate molecular weights. The advantage is that RI detector constant does not have to be known.

## EXPERIMENTAL

The chromatographic system consisted of a Waters 510 pump, an Ultrahydrogel Linear column or one or two Ultrastyragel Linear columns 300 × 7.8 mm

(Waters), a DAWN®-F laser photometer (Wyatt Technology Corporation), and a Wyatt Optilab 903 interferometric refractometer. Data were collected and handled by ASTRA® and EASI® software (Wyatt Technology Corporation). Tetrahydrofuran (THF) at a flow rate of 1 mL/min was used as a mobile phase for the Ultrastyragel column and 0.1 molar aqueous $Na_2SO_4$ with 0.04% $NaN_3$ (flow 0.5 mL/min) served as a mobile phase for the Ultra-hydrogel column.

To check the accuracy of the instrument and to show various possible applications of the method, the following materials were analyzed:

- Narrow polystyrene (PS) standards (Waters, Polymer Laboratories, Pressure Chemicals Co.).
- Broad PS standards (NBS 706, Aldrich Cat. No. 18243–5, Lot. No. 3507kk).
- Narrow polymethylmethacrylate (PMMA) standards (Polymer Laboratories).
- Broad PMMA (SYNPO).
- Pullulan standard P400 (Shodex).
- Alkyd resin (SYNPO).
- Phenoxy resins (Union Carbide).
- Derivatized (THF soluble) and underivatized (water soluble) polyvinylsugars (Institute for Organic and Macromolecular Chemistry, Düsseldorf). For detailed description of these polymers see ref. 11.

The DAWN photometer (operating at 633 nm) was calibrated using toluene and Rayleigh ratio 1.406 $\times$ $10^{-5}$ $cm^{-1}$. Normalization of the instrument was carried out by PS standard of molecular weight 200,000 and pullulan standard P400 using RMS radii 18 and 23 nm, respectively.[12,13] The $dn/dc$ calculation method was employed for the analysis of PS, PMMA, and phenoxy resins using the following dn/dc values: 0.1845 mL/g (PS),[10] 0.084 mL/g (PMMA),[9] 0.1773 mL/g (phenoxy resin).[10] The mass method was used for other polymers. RI detector was calibrated by aqueous NaCl solutions employing $dn/dc$ 0.174 mL/g. The following equations for $A_2$ of PS and PMMA were used for the determination of molecular weights and RMS radii of narrow PS and PMMA standards:

$$A_2(\text{PS}) = 0.01 \times M_w^{-0.25} \qquad (20)$$

$$A_2(\text{PMMA}) = 0.012 \times M_w^{-0.29} \qquad (21)$$

The equations were derived using data from ref. 14 (PS) and 15 (PMMA). For all other polymers (including broad PS and PMMA), the $A_2$ values were neglected. Literature values of the Mark-Houwink constants $a = 0.717$ and $K = 1.17 \times 10^{-2}$ mL/g were used for PS.[16] The Mark-Houwink coefficients of PMMA were provided by the determination of intrinsic viscosity of five narrow PMMA standards covering the molecular weight range of 64,000 to 1,300,000. The values are: $a = 0.70$ and $K = 1.07 \times 10^{-2}$ mL/g.

Using a 100 μL sample loop, the true injection volume was determined by the measurement of PS solutions of different concentrations and comparison of the injected masses with those calculated by the $dn/dc$ method. Sample concentrations were 0.04–0.3% w/v for narrow standards, 0.17% for PS, 0.35% for PMMA and polyvinylsugars, 0.6% for phenoxy resins, 0.9% for alkyd.
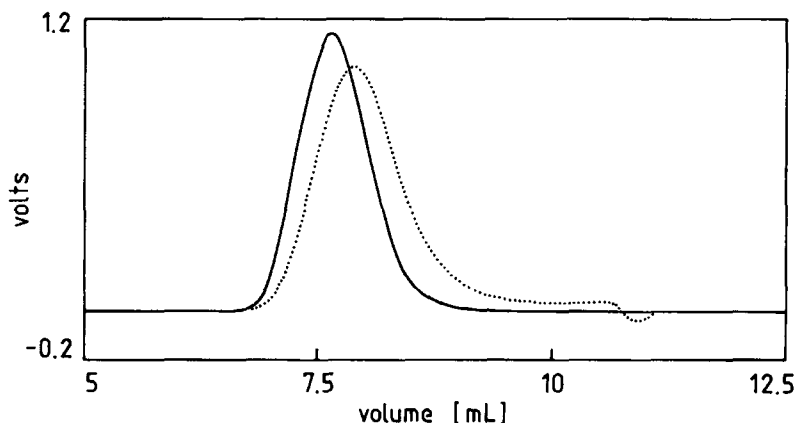


**Figure 1**   RI (dotted line) and 90° light scattering (full line) chromatograms of PS NBS 706.

**Table I   Slice-by-Slice Details from Two Sections of PS NBS 706 Chromatogram**

| Slice Index | Volume [mL] | Molecular weight | $\langle r_g^2 \rangle^{1/2}$ [nm] | Concentration [g/mL] |
|---|---|---|---|---|
| 344 | 7.16 | $8.99 \times 10^5$ | 41.9 | $2.74 \times 10^{-5}$ |
| 345 | 7.17 | $8.70 \times 10^5$ | 41.2 | $2.94 \times 10^{-5}$ |
| 346 | 7.18 | $8.36 \times 10^5$ | 40.7 | $3.14 \times 10^{-5}$ |
| 347 | 7.19 | $8.18 \times 10^5$ | 40.6 | $3.33 \times 10^{-5}$ |
| 348 | 7.20 | $8.10 \times 10^5$ | 40.0 | $3.48 \times 10^{-5}$ |
| 349 | 7.21 | $7.97 \times 10^5$ | 39.6 | $3.64 \times 10^{-5}$ |
| 350 | 7.22 | $7.89 \times 10^5$ | 39.7 | $3.81 \times 10^{-5}$ |
| 351 | 7.23 | $7.79 \times 10^5$ | 39.3 | $3.98 \times 10^{-5}$ |
| 352 | 7.24 | $7.68 \times 10^5$ | 38.6 | $4.15 \times 10^{-5}$ |
| 353 | 7.25 | $7.55 \times 10^5$ | 38.3 | $4.33 \times 10^{-5}$ |
| 354 | 7.26 | $7.48 \times 10^5$ | 38.2 | $4.51 \times 10^{-5}$ |
| 419 | 7.85 | $2.78 \times 10^5$ | 22.7 | $1.70 \times 10^{-4}$ |
| 420 | 7.86 | $2.75 \times 10^5$ | 22.6 | $1.70 \times 10^{-4}$ |
| 421 | 7.87 | $2.69 \times 10^5$ | 22.6 | $1.70 \times 10^{-4}$ |
| 422 | 7.88 | $2.65 \times 10^5$ | 22.1 | $1.71 \times 10^{-4}$ |
| 423 | 7.89 | $2.62 \times 10^5$ | 21.7 | $1.70 \times 10^{-4}$ |
| 424 | 7.90 | $2.58 \times 10^5$ | 21.6 | $1.70 \times 10^{-4}$ |
| 425 | 7.91 | $2.53 \times 10^5$ | 21.7 | $1.70 \times 10^{-4}$ |
| 426 | 7.92 | $2.48 \times 10^5$ | 21.7 | $1.70 \times 10^{-4}$ |
| 427 | 7.93 | $2.42 \times 10^5$ | 21.3 | $1.69 \times 10^{-4}$ |
| 428 | 7.94 | $2.38 \times 10^5$ | 20.9 | $1.69 \times 10^{-4}$ |
| 429 | 7.95 | $2.35 \times 10^5$ | 20.8 | $1.68 \times 10^{-4}$ |

## RESULTS AND DISCUSSION

### Determination of Molecular Weight

Figure 1 shows RI and MALLS (90°) detector profiles for PS NBS 706. The volume delay between the two detectors was determined by means of nearly monodisperse PS standard and corrected by the software. The two peaks do not overlap because of the different type of response of both detectors (the RI detector response is only proportional to the concentration, whereas the MALLS detector response is proportional to both the molecular weight and the concentration). Slice-by-slice details from two small sections of the NBS 706 chromatogram are shown in Table I. Table II lists molecular weight averages of three broad samples. As there is a simple relationship between the logarithm of molecular weight and GPC elution volume, the data from the higher concentration section of the peak may be extrapolated to the noisy edge sections as demonstrated in Figure 2 for a broad PS. The extrapolation reduces errors caused by low signal from detectors at the edges of distribution.

The influence of $A_2$ on the molecular weights of PS and PMMA standards is shown in Tables III and IV. It is common practice in GPC-MALLS and GPC-LALLS experiments to disregad the $A_2$ values, but the results in Tables III and IV clearly show that the deviation of $M_w$ may reach about 10% of the correct value. As ASTRA does not make it pos-

**Table II   Molecular Weight Averages of Broad Polymers**

| Sample | Nominal $M_n$ | Experimental $M_n$ | Nominal $M_w$ | Experimental $M_w$ |
|---|---|---|---|---|
| PS NBS 706 | 137,000 | 104,000 | 258,000[LS] | 277,000 |
| | | | 288,000[UC] | |
| PA Aldrich | 85,000[GPC] | 102,000 | 321,000[LS] | 322,000 |
| PMMA | 185,000[MO] | 160,000 | 494,000[GPC] | 517,000 |
| | 139,000[GPC] | | | |

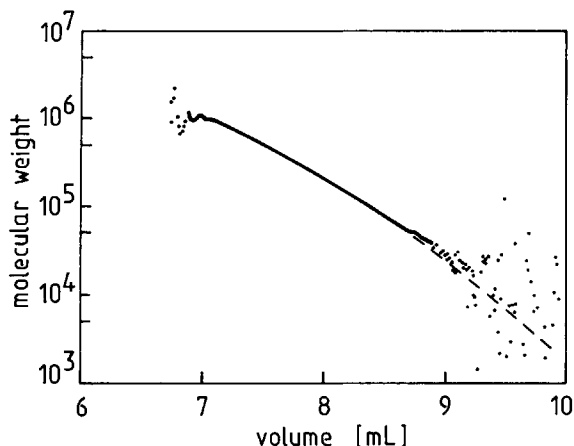LS: Light scattering, UC: Ultracentrifugation, MO: Membrane osmometry.

**Figure 2** Extrapolation of molecular weight vs. elution volume plot for PS NBS 706.

sible to change $A_2$ according to Eq. (4), an average value of $A_2$ must be used for broad samples.

Molecular weight vs. elution volume plot may provide some additional information about the polymer under investigation. Figure 3 contrasts the plots of broad PS and poly(vinyl isopropylidene arabinose ketone). Molecular weight of polyvinylsugar molecules is significantly higher compared with that of PS molecules of the same GPC elution volume (i.e., of the same hydrodynamic volume). The density of polyvinylsugar coils must be significantly higher than that of PS ones. The plots in Figure 3 also show that the application of conventional GPC with PS calibration would give quite missleading results. In the case of sample from Figure 3, $M_n$(GPC) = 190,000 and $M_w$(GPC) = 720,000, while $M_n$(GPC-MALLS) = 340,000 and $M_w$(GPC-MALLS) = 1,820,000.

The intensity of the scattered light can be expressed by two equations: (1) and (10). A first-order

polynomial is sufficient for the $R_\Theta/Kc$ vs. $\sin^2(\Theta/2)$ plot up to the molecular weight of about 500,000, but higher-order fits must be used for high molecular weights (Fig. 4). Figure 5 presents $Kc/R_\Theta$ vs. $\sin^2(\Theta/2)$ plot for the same slice as in Figure 4 and shows that the plot is linear even for the high molecular weight. The comparison of both plots (Tables V and VI) shows good agreement of the molecular weights and RMS radii up to the values of about 2,000,000 and 60 nm, respectively. The linearity of $Kc/R_\Theta$ plot over a broad range of molecular weight is a great advantage because the use of $R_\Theta/Kc$ plot for broad distribution samples may require different polynomial orders to fit the light scattering data in different parts of a chromatogram.

## Determination of Molecular Size

RMS radius is another important physical quantity accessible from the GPC-MALLS experiments. Tables V and VI schedule RMS radii of PS and PMMA in THF at ambient temperature determined by $R_\Theta/Kc$ vs. $\sin^2(\Theta/2)$ and $Kc/R_\Theta$ vs. $\sin^2(\Theta/2)$ plots. As the RMS radius is determined from the slope of angular dependence of the scattered light intensity near the origin, the precision of the size determination is strongly dependent on the signal-to-noise ratio. The results shown in Tables V and VI were obtained using the middle slices of the peaks of narrow standards in order to improve the precision of the measurement. To verify the accuracy of obtained values, the GPC-MALLS results were compared with those calculated from Flory-Fox and Ptitsyn-Eizner equations:[17,18]

$$\langle r_g^2 \rangle^{1/2} = \frac{1}{\sqrt{6}} \left( \frac{[\eta] M}{\Phi} \right)^{1/3} \tag{22}$$

**Table III   The Influence of the Second Virial Coefficient on the Molecular Weights of PS Standards**

| Injected concentration [%] | Concentration at the top of peak $10^4$ [g/mL] | $M_w$ using $A_2$ according to Eq. (20) | $M_w$ using $A_2$ = 0 | $M_w$ using $A_2$ = 0 (% of correct value) |
|---|---|---|---|---|
| 0.20 | 5.05 | 34,700 | 34,000 | 98.0 |
| 0.10 | 2.66 | 96,000 | 94,000 | 97.9 |
| 0.08 | 2.31 | 202,000 | 194,000 | 96.0 |
| 0.07 | 1.78 | 455,000 | 431,000 | 94.7 |
| 0.07 | 1.51 | 852,000 | 793,000 | 93.1 |
| 0.07 | 1.49 | 1,068,000 | 979,000 | 91.7 |
| 0.04 | 0.78 | 1,667,000 | 1,558,000 | 93.5 |
| 0.04 | 0.73 | 3,339,000 | 2,986,000 | 89.4 |

**Table IV    The Influence of the Second Virial Coefficient on the Molecular Weights of PMMA Standards**

| Injected concentration [%] | Concentration at the top of peak $10^4$ [g/mL] | $M_w$ using $A_2$ according to Eq. (21) | $M_w$ using $A_2 = 0$ | $M_w$ using $A_2 = 0$ (% of correct value) |
|---|---|---|---|---|
| 0.30 | 6.87 | 63,000 | 61,000 | 96.8 |
| 0.25 | 6.02 | 119,000 | 113,000 | 95.0 |
| 0.15 | 3.84 | 199,000 | 190,000 | 95.5 |
| 0.15 | 3.10 | 268,000 | 256,000 | 95.5 |
| 0.15 | 3.76 | 423,000 | 391,000 | 92.4 |
| 0.15 | 3.17 | 716,000 | 653,000 | 91.2 |
| 0.15 | 2.59 | 831,000 | 762,000 | 91.7 |
| 0.15 | 2.08 | 1,351,000 | 1,220,000 | 90.3 |

$$\Phi = 2.86 \times 10^{21} (1 - 2.63\varepsilon + 2.86\varepsilon^2) \quad (23)$$

$$\varepsilon = \frac{2a - 1}{3} \quad (24)$$

where $a$ is the exponent of the Mark-Houwink equation:

$$[\eta] = KM^a \quad (25)$$

where $K$ and $a$ are constants for a given polymer, solvent, and temperature. Using $[\eta]$ in dL/g, Eq. (22) gives RMS radii in cm. The deviations of experimental RMS radii (obtained by $R_\Theta/Kc$ plot) from Flory-Fox theoretical values are less than 10%. Yau and Rementer[19] published that ". . . there appears to be a narrow window in which reliable $\langle r_g^2 \rangle^{1/2}$ values can be obtained by GPC-MALLS technology. The lower limit is approximately 10 nm, which corresponds roughly to a $M_w$ value of 100,000 PS, and the upper value is about 30 nm correspond-



**Figure 3**    Molecular weight vs. elution volume plots of PS (●) and poly(vinyl isopropylidene arabinose ketone) (○).

ing to 500,000 PS." The results presented in Tables V and VI clearly show that there is no narrow window. Naturally, there is a lower limit of about 10 nm where $P(\Theta)$ approaches unity.

Data from Tables V and VI ($R_\Theta/Kc$ plots) give the following relationships between the molecular weight and RMS radius of PS and PMMA in THF at ambient temperature:

$$\text{PS:} \langle r_g^2 \rangle^{1/2} = 0.014 \times M^{0.585} \quad (26)$$

$$\text{PMMA:} \langle r_g^2 \rangle^{1/2} = 0.012 \times M^{0.583} \quad (27)$$

Figures 6 and 7 present the log-log plots of RMS radius vs. molecular weight for PS and PMMA generated by GPC-MALLS analysis of broad samples using EASI software. The slopes fit well with the typical values for random coils (0.5–0.6). Figure 8 presents the same plot for branched polymer (alkyd resin). The slope of 0.38 corresponds to branched molecules.

RMS radius of a broad sample can be plotted as a function of elution volume and extrapolated by the same procedure as in the case of molecular weight. Consequently, the RMS radii that are unaccessible experimentally due to lower molecular size or detector response may be estimated and RMS radius distribution together with its various moments can be determined. For example, the RMS radius averages of PS NBS 706 are as follows:

$$\langle r_g^2 \rangle_n^{1/2} = 12 \text{ nm}, \quad \langle r_g^2 \rangle_w^{1/2} = 23 \text{ nm}, \quad \text{and}$$
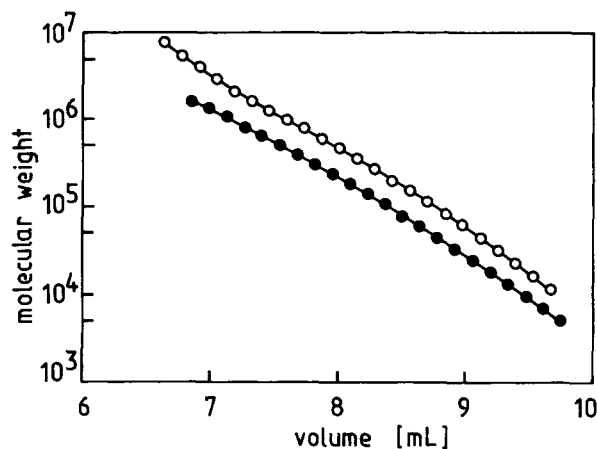
$$\langle r_g^2 \rangle_z^{1/2} = 29 \text{ nm}.$$

## Characterization of Branching

For a couple of linear and branched polymers of the same chemical composition, the branching ratio:[20]
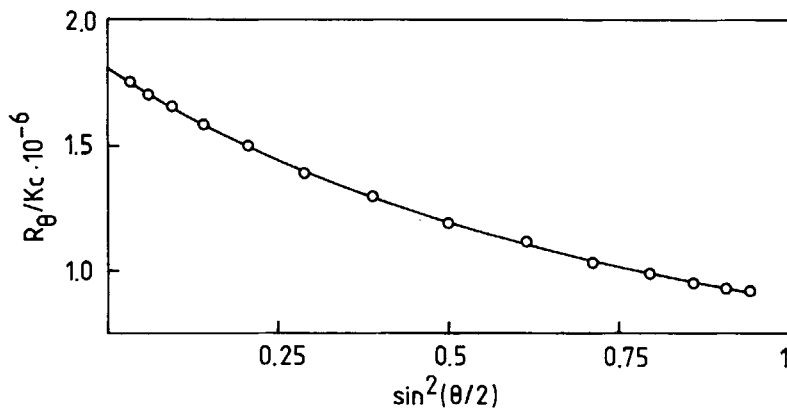
**Figure 4**   $R_\Theta/Kc$ vs. $\sin^2(\Theta/2)$ plot of a single slice from the chromatogram top of PS standard of molecular weight 1,840,000. Third-order fit.

$$g_M = \frac{\langle r_g^2 \rangle_{\mathrm{br}}}{\langle r_g^2 \rangle_{\mathrm{lin}}} \qquad (28)$$

can be determined as a function of molecular weight. The subscripts br and lin refer to branched and linear molecules. The parameter $g_M$ compares the MS radius of the branched and linear molecules of the identical molecular weight, and as the branched molecules are more compact than corresponding linear molecules, the parameter is always less than 1. The determination of the relation between $g_M$ and molecular weight represents a very sophisticated description of branched polymers, but the suitable linear counterpart is not often available. In many practical cases the polymer sample can contain branched species as a consequence of side reactions (e.g., chain transfer to polymer) and the actual analytical task is to prove the presence of branched molecules.

Information about the conformation of polymer chain can be inferred from RMS radius vs. molecular

weight plot. A slope of 0.5 to 0.6 (see Figs. 6 and 7) corresponds to the linear random coils. A slope less than 0.5 (see Fig. 8) hints the presence of branched molecules (0.33 for spheres), while higher values are indicative of rod-like polymer chain arrangement (1 for rods). A good detector signal over a broad range of molecular weight is necessary to get reliable slope. The accuracy of the slope may be affected by nonsize exclusion mechanisms (e.g., adsorption) that can delay some molecules. Due to this effect, the slices of higher elution volume can contain a mixture of molecules of lower molecular weight (separated by pure size exclusion) and molecules of higher molecular weight that were retained by the nonsize exclusion mechanisms and the slope is underestimated since $z$ averages of RMS radius are related with weight averages of molecular weight. Nonsize exclusion effects may be frequent in aqueous GPC.

Other possibility of the identification of branched molecules is log-log intrinsic viscosity vs. molecular weight plot. For polymers obeying the universal cal-
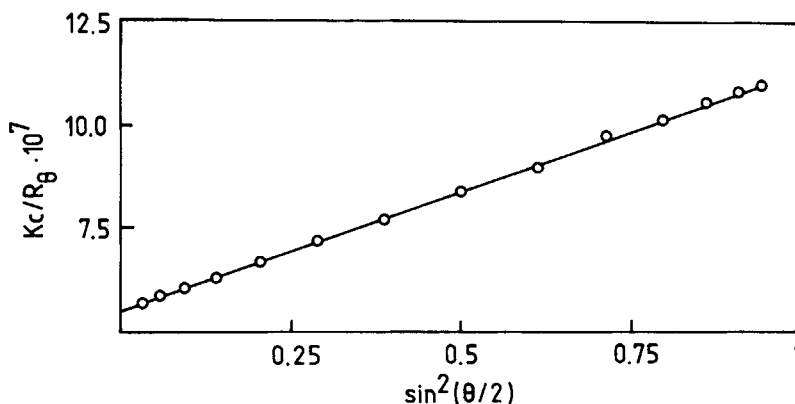


**Figure 5**   $Kc/R_\Theta$ vs. $\sin^2(\Theta/2)$ plot of the same slice as in Figure 4. First-order fit.

**Table V RMS Radii of PS in THF at Ambient Temperature**

| Flory-Fox $\langle r_g^2 \rangle^{1/2}$ [nm] | $R_\theta/Kc$ Plot $M$ | $R_\theta/Kc$ Plot $\langle r_g^2 \rangle^{1/2}$ [nm] | $R_\theta/Kc$ Plot Fit Order | $Kc/R_\theta$ Plot Fit Order | $Kc/R_\theta$ Plot $M$ | $Kc/R_\theta$ Plot $\langle r_g^2 \rangle^{1/2}$ [nm] |
|---|---|---|---|---|---|---|
| 12.0 | 105,000 | 12.3 | 1 | 1 | 104,000 | 12.5 |
| 13.5 | 130,000 | 13.7 | 1 | 1 | 130,000 | 13.9 |
| 18.4 | 222,000 | 18.2 | 1 | 1 | 222,000 | 18.9 |
| 26.5 | 422,000 | 24.6 | 1 | 1 | 421,000 | 26.3 |
| 29.7 | 513,000 | 29.4 | 2 | 1 | 510,000 | 28.7 |
| 36.4 | 733,000 | 37.1 | 2 | 1 | 729,000 | 37.0 |
| 41.0 | 902,000 | 41.9 | 2 | 1 | 895,000 | 42.0 |
| 46.3 | 1,116,000 | 49.3 | 3 | 1 | 1,107,000 | 49.0 |
| 58.2 | 1,667,000 | 59.0 | 3 | 1 | 1,667,000 | 61.5 |
| 63.0 | 1,915,000 | 65.5 | 3 | 1 | 1,917,000 | 68.0 |
| 74.0 | 2,534,000 | 79.7 | 3 | 1 | 2,612,000 | 91.5 |
| 98.3 | 4,161,000 | 100.5 | 3 | 1 | 4,363,000 | 122.1 |

ibration (based on the calibration parameter $[\eta]M$),[21] the intrinsic viscosity can be gained using universal calibration, i.e., $\log([\eta]M)$ vs. elution volume relationship. The universal calibration can be produced using narrow standards (or a broad polymer sample) with reliably known Mark-Houwink coefficients. As the light scattering detector measures molecular weight at each volume slice, the value of intrinsic viscosity for each slice may be read from $\log([\eta]M)$ vs. elution volume calibration curve and the intrinsic viscosity distribution and intrinsic viscosity averages can be determined. Determination of the intrinsic viscosity by GPC with a light scattering detector is absolutely identical with the determination of the molecular weight by GPC equipped with a viscometric detector where the intrinsic viscosity is the measured quantity and the molecular weight is calculated from the universal calibration curve. Figure 9 relates the intrinsic viscosity and the molecular weight of broad PMMA sample. The linear plot corresponds to the linear random coils. The slope of the plot (the exponent

of the Mark-Houwink equation) is 0.72, which is close to the exponent obtained by classical procedure (see Experimental section). The same plot for two samples of phenoxy resin is shown in Figure 10. The deviation from the linearity gives evidence about the presence of branched molecules in both samples. Compared to the RMS radius vs. molecular weight plot, this is also applicable to lower molecular weight samples where the determination of RMS radii is uncertain or impossible.

The sizes of the macromolecules of branched polymers are smaller than those of the macromolecules of linear polymers of the same molecular weight. As GPC elution volume depends on the molecular size, the comparison of the molecular weight vs. elution volume plots of samples of the identical chemical composition may reveal branching.

Figure 11 presents molecular weight vs. elution volume plots of two samples of poly(vinyl galactose ketone). The plots overlap in the region of molecular weight below about 1,000,000. The deviation of the curves above this limit suggests that the sample (●)

**Table VI RMS Radii of PMMA in THF at Ambient Temperature**

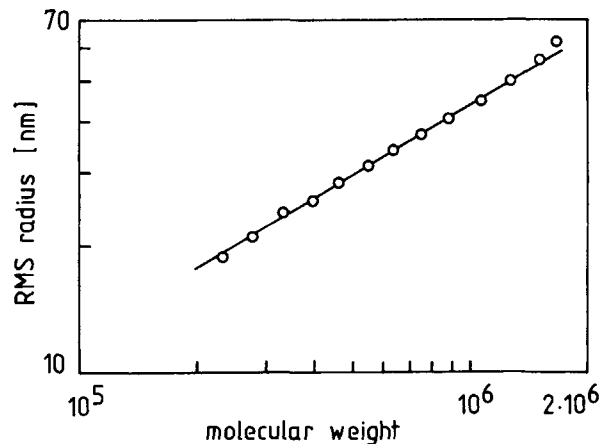| Flory-Fox $\langle r_g^2 \rangle^{1/2}$ [nm] | $R_\theta/Kc$ Plot $M$ | $R_\theta/Kc$ Plot $\langle r_g^2 \rangle^{1/2}$ [nm] | $R_\theta/Kc$ Plot Fit Order | $Kc/R_\theta$ Plot Fit Order | $Kc/R_\theta$ Plot $M$ | $Kc/R_\theta$ Plot $\langle r_g^2 \rangle^{1/2}$ [nm] |
|---|---|---|---|---|---|---|
| 12.2 | 131,000 | 12.7 | 1 | 1 | 130,000 | 13.2 |
| 16.0 | 211,000 | 16.9 | 1 | 1 | 212,000 | 17.4 |
| 19.3 | 294,000 | 18.3 | 1 | 1 | 294,000 | 19.2 |
| 24.8 | 456,000 | 22.8 | 1 | 1 | 453,000 | 24.2 |
| 32.7 | 744,000 | 30.0 | 1 | 1 | 741,000 | 33.1 |
| 35.7 | 870,000 | 37.2 | 2 | 1 | 860,000 | 36.6 |
| 47.4 | 1,434,000 | 51.9 | 2 | 1 | 1,423,000 | 54.2 |
| 55.9 | 1,919,000 | 59.6 | 3 | 1 | 1,922,000 | 62.7 |

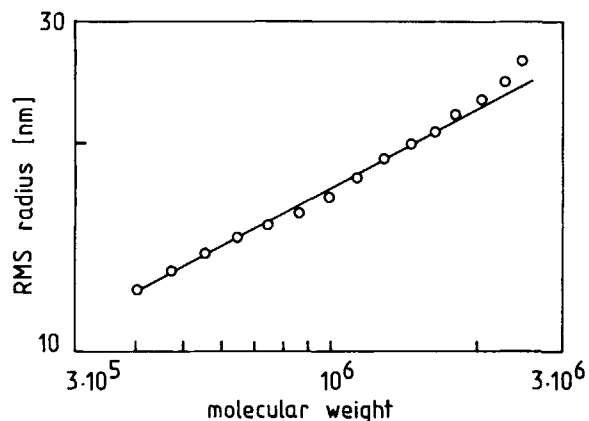**Figure 6** RMS radius vs. molecular weight plot for PS, slope = 0.56.



**Figure 8** RMS radius vs. molecular weight plot for alkyd resin, slope = 0.38.

contains at the high molecular weight region more branched molecules than the sample (O).

Figure 12 shows the molecular weight vs. elution volume plots of two samples of poly(3-O-methacryloyl gluconic acid) including RI chromatograms. The shift of both plots may be explained by the expressive branching of the sample (●). It is important to note that the chromatogram of the sample (O) is shifted towards lower elution volumes and, therefore, conventional GPC would evaluate the sample (●) as one with lower molecular weight, whereas the opposite fact is true.

If a linear standard of the same chemical structure and the molecular weight range is available, the branching parameter can be calculated using equation:[22]

$$g_M = \left(\frac{M_{lin}}{M_{br}}\right)_V^{(a+1)/e} \qquad (29)$$

where $M_{lin}$ and $M_{br}$ are molecular weights of linear and branched polymer, respectively, $V$ denotes common elution volume, $a$ is the Mark-Houwink exponent for the linear polymer, and $e$ is the drainage parameter, ranging from 0.5 to 1.5.[23]

Figure 13 shows another interesting example. Shown here are chromatograms of the MALLS (90°) and RI detectors of a sample of poly(2-(D-glucopyranosyl-3-oxymethyl)-acrylic acid ethyl ester). The light scattering chromatogram shows two peak maxima, while only one maximum is recorded by RI detector. The peak at the lower elution volume at the light scattering chromatogram may be ex-
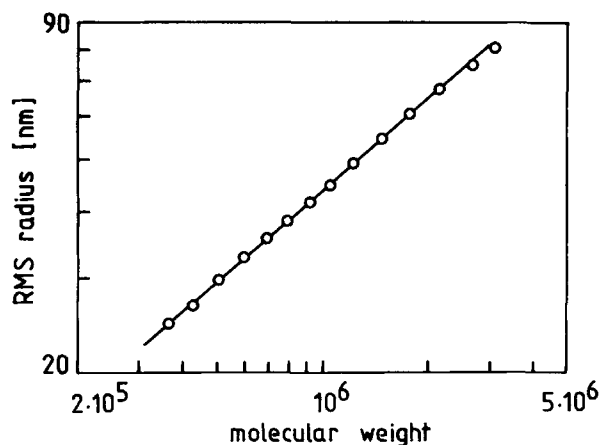


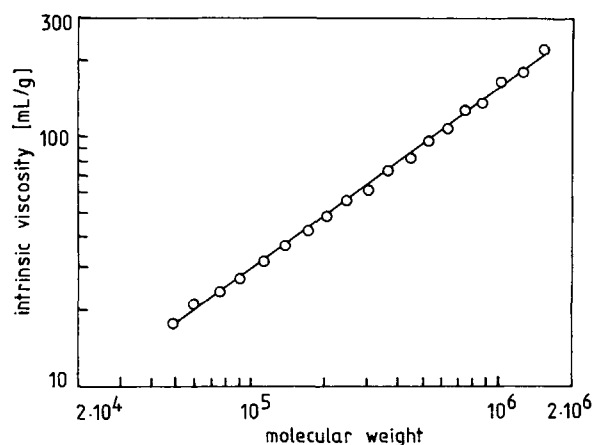**Figure 7** RMS radius vs. molecular weight plot for PMMA, slope = 0.57.



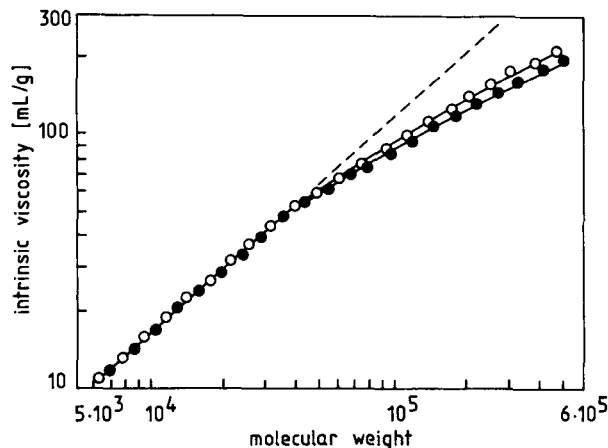**Figure 9** Intrinsic viscosity vs. molecular weight plot of PMMA.

**Figure 10**  Intrinsic viscosity vs. molecular weight plots of two phenoxy resins: UCAR PKHC (O), UCAR PKHJ (●).
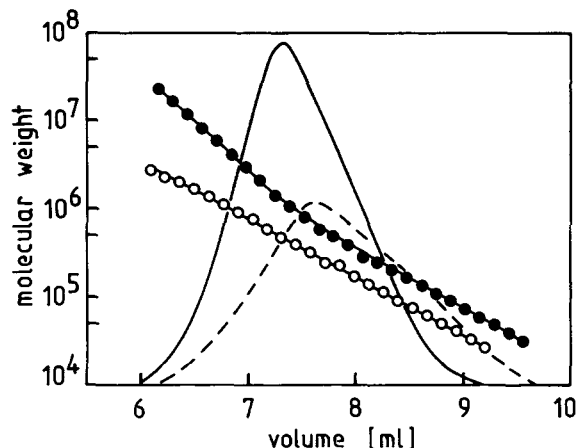


**Figure 12**  Molecular weight vs. elution volume plots of two samples of poly(3-O-methacryloyl gluconic acid) with RI chromatograms superimposed; ● dashed line, O full line.

plained by the presence of highly branched molecules or supermolecular aggregates. The concentration of these species is very low, as can be seen from the signal of RI detector.

## Comparison of GPC-MALLS with the Relative Methods

Classical light scattering technique provides the weight-average molecular weight, $z$ average RMS radius and $A_2$, but no information about the molecular weight and size distribution. The possibilities of branching characterization are strongly limited because $M_w$ and $\langle r_g^2 \rangle_z^{1/2}$ can be compared only for monodisperse samples. The results may be distorted



**Figure 11**  Molecular weight vs. elution volume plots of two poly(vinyl galactose ketone) samples.

by the presence of dust particles, microgels, or supermolecular aggregates. The advantage of the method is no shearing degradation of high molecular weight fractions in the GPC instrument.

GPC-LALLS cannot provide RMS radius information because no angular variation of scattered light intensity is measured.

GPC, coupled with a viscometric detector, measures the distribution of intrinsic viscosity. In order to obtain molecular weight distribution the columns must be calibrated by standards of known molecular weight to obtain $\log([\eta]M)$ vs. elution volume universal calibration. The universal calibration approach is highly sensitive to various mechanisms other than pure size exclusion during the chromatographic separation.

Conventional GPC, using a concentration detector, only may remain a widely employed technique of polymer characterization because the MALLS photometer constitutes a substantial amount of the purchase price of the GPC-MALLS instrument. The method can give accurate molecular weight distribution of linear polymers for which either well-characterized standards or reliable Mark-Houwink constants are available. For linear polymers with no standards or Mark-Houwink coefficients, apparent molecular weight distribution and molecular weight averages can be determined using polystyrene calibration. These data may be useful for the comparison of different samples of a given polymer. Even simple graphical comparison of GPC chromatograms may provide valuable information about the influence of the reaction conditions on the molecular
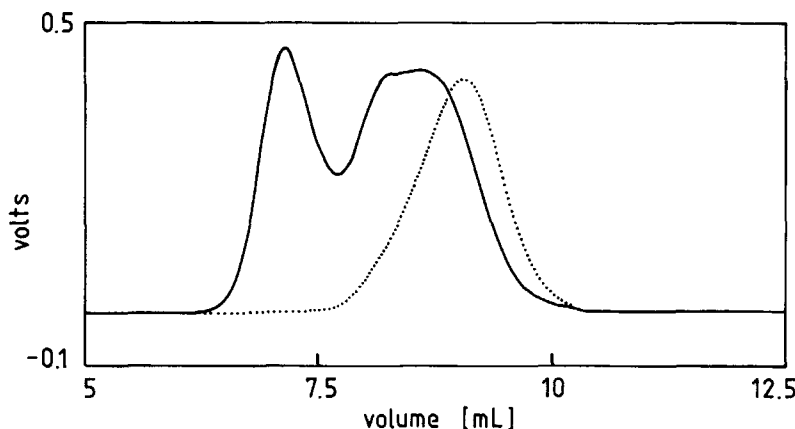
**Figure 13**   RI (dotted line) and 90° light scattering (full line) chromatograms of poly(2-(D-glucopyranosyl-3-oxymethyl)-acrylic acid ethyl ester).

weight distribution of products or about production reproducibility. The greatest failure of conventional GPC should be expected in the case of branched polymers where completely missleading results may be obtained.

## CONCLUSIONS

The combination of GPC with MALLS photometer enables:

- Absolute determination of the molecular weight distribution and molecular weight averages without column calibration.

- Determination of the RMS radius distribution and its various moments.

- For samples obeying the universal calibration, determination of the intrinsic viscosity distribution and the coefficients of the Mark-Houwink equation.

- Characterization of branching using the RMS radius vs. molecular weight, intrinsic viscosity vs. molecular weight, and molecular weight vs. elution volume plots. Determination of the branching parameter $g_M$ as a function of molecular weight.

- Highly sensitive determination of even minute amount of fractions with very high molecular weight.

- Investigation of the instrumental broadening and the shearing degradation in the GPC instrument.[24,25]

- Information useful for the interpretation of the results obtained by conventional GPC.

## REFERENCES

1. P. Debye, *J. Appl. Phys.*, **15**, 338 (1944).
2. B. H. Zimm, *J. Chem. Phys.*, **13**, 141 (1945).
3. B. H. Zimm, *J. Chem. Phys.*, **16**, 1093 (1948).
4. P. J. Wyatt, *Anal. Chim. Acta*, **272**, 1 (1993).
5. P. Kratochvíl, *Classical Light Scattering from Polymer Solutions, Polymer Science Library*, A. D. Jenkins (editor), Elsevier, Amsterdam, 1987.
6. C. Jackson and W. W. Yau, *J. Chromatogr.*, **645**, 209 (1993).
7. O. Procházka and P. Kratochvíl, *J. Appl. Polym. Sci.*, **31**, 919 (1986).
8. O. Procházka and P. Kratochvíl, *J. Appl. Polym. Sci.*, **34**, 2325 (1987).
9. *Polymer Handbook* (3rd ed.), J. Brandrup and E. H. Immergut, Eds., John Wiley and Sons, New York, 1989.
10. Chromatix Application Notes #1 and #2.
11. G. Wulff, J. Schmid, and T. Venhoff, in *Carbohydrates as Organic Raw Materials*, F. W. Lichtenthaler, Ed., VCH, Weinheim 1991, p. 311.
12. P. J. Wyatt, *J. Liquid Chromatogr.*, **14**, 2351 (1991).
13. C. Jackson, L. M. Nilsson, and P. J. Wyatt, *J. Appl. Polym. Sci.: Appl. Polym. Symp.*, **43**, 99 (1989).
14. G. V. Schulz and H. Baumann, *Makromol. Chem.*, **114**, 122 (1968).

15. G. V. Schulz, H. Baumann, and R. Darskus, *J. Phys. Chem.*, **70**, 3647 (1966).

16. M. Kolínský and J. Janča, *J. Polym. Sci.: Polym. Chem. Ed.*, 12, 1181 (1974).

17. T. G. Fox and P. J. Flory, *J. Am. Chem. Soc.*, **73**, 1904 (1951).

18. O. B. Ptitsyn and Yu. E. Eizner, *Sov. Phys. Tech. Phys.*, **4**, 1020 (1960).

19. W. W. Yau and S. W. Rementer, *J. Liquid Chromatogr.*, **13**, 627 (1990).

20. B. H. Zimm and W. H. Stockmayer, *J. Chem. Phys.*, **17**, 1301 (1949).

21. Z. Grubisic, P. Rempp, and H. Benoit, *J. Polym. Sci.: Polym. Lett. Ed.*, **5**, 753 (1967).

22. L. P. Yu and J. E. Rollings, *J. Appl. Polym. Sci.*, **33**, 1909 (1987).

23. B. H. Zimm and R. W. Kilb, *J. Polym. Sci.*, **37**, 19 (1959).

24. P. J. Wyatt, *J. Chromatogr.*, **648**, 27 (1993).

25. W. G. Rand and A. K. Mukherji, *J. Polym. Sci.: Polym. Lett. Ed.*, **20**, 501 (1982).